7 GHz resolution waveguide THz spectroscopy of explosives related solids showing new features

N. Laman,[1] S. Sree Harsha,[1] D. Grischkowsky,[1,*] and Joseph S. Melinger[2,3]

[1]*School of Electrical and Computer Engineering, Oklahoma State University, Stillwater, OK 74078, USA*
[2]*Naval Research Laboratory, Electronics Science and Technology Division, Code 6812, Washington, D.C. 20375, USA*
[3]*email: joseph.melinger@nrl.navy.mil*
[*]*Corresponding author: daniel.grischkowsky@okstate.edu*

Abstract: The vibrational modes of the explosive related solids 2,4- and 2,6-DNT have been measured with waveguide THz time-domain spectroscopy (THz-TDS) to unprecedented precision. Dramatic sharpening of spectral features upon cooling beyond 80 K to 12 K is observed, illustrating the high quality and alignment of the polycrystalline thin films. Many of the observed features have linewidths below 15 GHz. These linewidths are approximately 8 times narrower than for the corresponding measurements via conventional THz-TDS with cooled pellets. For the 2,4-DNT, the line narrowing resolved 19 absorption features compared to only 7 features with the corresponding pellet measurement.

OCIS codes: (130.2790) Guided waves; (160.4890) Organic materials; (300.6495) Spectroscopy, terahertz; (300.3700) Linewidth.

References and links

1. M. C. Kemp, P. F. Taday, B. E. Cole, J. A. Cluff, A. J. Fitzgerald, and W. R. Tribe, "Security applications of terahertz technology," Proc. SPIE **5070**, 44-52 (2003).
2. J. F. Federici, B. Schulkin, F. Huang, D. Gary, R. Barat, F. Oliveira, and D. Zimdars, "THz imaging and sensing for security applications – explosives, weapons and drugs," Semicond. Sci. Technol. **20**, S266-S280 (2005).
3. H.-B. Liu, H. Zhong, N. Karpowicz, Y. Chen, X.-C. Zhang, "Terahertz spectroscopy and imaging for defense and security applications," Proc. IEEE **95**, 1514-1527 (2007).
4. K. Yamamoto, M. Yamaguchi, F. Miyamaru, M. Tani, M. Hangyo, T. Ikeda, A. Matsushita, K. Koide, M. Tatsuno, and Y. Minami, "Noninvasive inspection of C-4 explosive in mails by terahertz time-domain spectroscopy," Jpn. J. Appl. Phys. **43**, L414-417 (2004).
5. T. Lo, I. S. Gregory, C. Baker, P. F. Taday, W. R. Tribe, and M. C. Kemp, "The very far-infrared spectra of energetic materials and possible confusion materials using terahertz pulsed spectroscopy," Vib. Spectrosc. **42,** 243-248 (2006).
6. J. Chen, Y. Chen, H. Zhao, G. J. Bastiaans, and X.-C. Zhang, "Absorption coefficients of selected explosives and related compounds in the range of 0.1-2.8 THz," Opt. Express **15**, 12060 (2007).
7. Y. Chen, H. Liu, and X.-C. Zhang, "THz spectra of 4-NT and 2,6-DNT," Proc. SPIE **6212**, 62120P (2006).
8. Y. Chen, H. Liu, Y. Deng, D. Schauki, M. J. Fitch, R. Osiander, C. Dodson, J. B. Spicer, M. Shur, and X.-C. Zhang, "THz spectroscopic investigation of 2,4-dinitrotoluene," Chem. Phys. Lett. **400**, 357-361 (2004).
9. Y. Hu, P. Huang, L. Guo, X. Wang, C. Zhang, "Terahertz spectroscopic investigations of explosives," Phys. Lett. A **359**, 728-732 (2006).
10. M. R. Leahy-Hoppa, M. J. Fitch, X. Zheng, L. M. Hayden,and R. Osiander, "Wideband terahertz spectroscopy of explosives," Chem. Phys. Lett. **434**, 227-230 (2007).
11. A.D. Burnett, W.H. Fan, P.C. Upadhya, J.E. Cunningham, H.G.M. Edwards, J. Kendrick, T. Munshi, M. Hargreaves, E.H. Linfield, A.G. Davies, "Broadband terahertz time-domain and Raman spectroscopy of explosives," Proc. SPIE **6549**, 654905 (2007).
12. W. H. Fan, A. Burnett, P. C. Upadhya, J. Cunningham, E. H. Linfield, and A. G. Davies, "Far-infrared spectroscopic characterization of explosives for security applications using broadband terahertz time-domain spectroscopy," Appl. Spectrosc. **61**, 638-643 (2007).
13. J. Barber, D. E. Hooks, D. J. Funk, R. D. Averitt, A. J. Taylor, D. Babikov, "Temperature-dependent far-infrared spectra of single crystals of high explosives using terahertz time-domain spectroscopy," J. Phys. Chem. A **109**, 3501-3505 (2005).

#92514 - $15.00 USD Received 6 Feb 2008; revised 7 Mar 2008; accepted 7 Mar 2008; published 11 Mar 2008

14. R. J. Foltynowicz, R. E. Allman, and E. Zuckerman, "Terahertz absorption measurement for gas-phase 2,4-dinitrotoluene from 0.05 THz to 2.7 THz," Chem. Phys. Lett. **431**, 34-38 (2006).
15. J. Zhang and D. Grischkowsky, "Waveguide THz time-domain spectroscopy of nm water layers," Opt. Lett. **19**, 1617-1619 (2004).
16. J. S. Melinger, N. Laman, S. S. Harsha, and D. Grischkowsky, "Line narrowing of terahertz vibrational modes for organic thin polycrystalline films within a parallel plate waveguide," Appl. Phys. Lett. **89**, 251110 (2006).
17. R. Mendis and D. Grischkowsky, "Undistorted guided wave propagation of sub-picosecond THz pulses," Opt. Lett. **26**, 846-848 (2001).
18. G. Gallot, S. P. Jamsion, R. W. McGowan, and D. Grischkowsky, "THz Waveguides," J. Opt. Soc. Am. B **17**, 851-863 (2000).
19. J. S. Melinger, N. Laman, S. S. Harsha, S. Cheng, and D. Grischkowsky, "High-resolution waveguide terahertz spectroscopy of partially oriented organic polycrystalline films," J. Phys. Chem. A **111**, 10977-10987 (2007).
20. N. Laman, S. S. Harsha, D. Grischkowsky, and J. S. Melinger, "High resolution waveguide THz spectroscopy of biological molecules," Biophys. J. **94**, 1010-1020 (2008).
21. N. Laman, S. S. Harsha, and D. Grischkowsky, "Narrow-line waveguide terahertz time-domain spectroscopy of aspirin and aspirin precursors," Appl. Spectrosc. **62**, 319-326 (2008).
22. J.P. Pinan, R. Ouillon, P. Ranson, M. Becucci, S. Califano, "High resolution Raman study of phonon and vibron bandwidths in isotopically pure and natural benzene crystal," J. Chem. Phys. **109**, 5469-5480 (1998).
23. D. Grischkowsky, S. Keiding, M. van Exter, Ch. Fattinger, "Far-infrared time-domain spectroscopy with terahertz beams of dielectrics and semiconductors," J. Opt. Soc. Am. B **7**, 2006-2015 (1990).
24. M. van Exter and D. Grischkowsky, "Characterization of an optoelectronic terahertz beam system," IEEE Trans. Microwave Theory Tech. **38**, 1684-1691 (1990).
25. W. C. McCrone and S.-M. Tsang, "Crystallographic Data. 88. 2,4-Dinitrotoluene," Anal. Chem. **26**, 1848-1849 (1954).
26. P. U. Jepsen and S. J. Clark, "Precise ab-initio prediction of terahertz vibrational modes in crystalline systems," Chem. Phys. Lett. **442**, 275-280 (2007).
27. D. G. Allis, D. A. Prokhorova, and T. M. Korter, "Solid state modeling of the terahertz spectrum of the high explosive HMX," J. Phys. Chem. A **110**, 1951-199 (2006).
28. J.-J. Nie, D.-J. Xu, Z.-Y. Li, and M. Y. Chaing, "2,6-Dinitrotoluene," Acta. Crystallogr. **E57**, o827 (2001).

1. Introduction

One of the most promising and discussed [1-4] applications of THz time-domain spectroscopy (THz-TDS) is the detection and identification of explosive materials. The absorption spectra of a number of explosives and related compounds have been measured previously by a number of different groups [1-13]. While these measurements are important to determine the feasibility of standoff explosive detection, the solid explosives are only identified by a few broad, overlapping lines. In order precisely identify and distinguish explosives, one must acquire spectra at the highest possible resolution, resolving a large number of absorption features which can be used as a unique 'spectral fingerprint'.

The majority of the previous work [1-10] has been performed using THz-TDS to measure sample pellets at room temperature. A notable exception is the recent work by the group at the University of Leeds [11, 12] reporting observations on pellets cooled to 4 K. In addition, the group at Los Alamos National Laboratory [13] measured the THz absorption of difficult to manufacture single crystals of explosives. All of these pellets are formed under pressure from a polycrystalline powder of the sample, either singly or with a transparent powder host such as polyethylene. The inherent disorder of the random orientations and sizes of the constituent crystals, as well as possible interactions with the host material under pressure, introduces a great degree of inhomogeneous broadening to the THz absorption features. This broadening, combined with the homogeneous broadening due to energy relaxation, pure dephasing, and thermal excitation of the vibrational coordinates, broadens the underlying THz spectrum and obscures many features. While the gas-phase work on 2,4-DNT by Foltynowicz and coworkers [14] have many narrow spectral lines, these are mainly due to rotational motions and can not be compared to the work presented here.

In order to increase the sensitivity and resolution compared to THz-TDS characterization of pellets, our group has developed the technique of waveguide THz-TDS [15, 16]. Here, a thin film of the material under study is formed on a metal plate. This plate is subsequently

#92514 - $15.00 USD Received 6 Feb 2008; revised 7 Mar 2008; accepted 7 Mar 2008; published 11 Mar 2008

incorporated in a single-mode parallel plate waveguide [17], similar to microwave parallel-plate waveguides, but with the dimensions of the gap scaled down to 50 μm to correspond with the smaller wavelength. The THz radiation is coupled into and out of the gap via high-resistivity Si lenses. The guided THz propagates along, and is partially absorbed by, the sample film. The confinement of the THz radiation to a gap of size b, combined with the long interaction length corresponding to the waveguide length L, results in an improvement of the sensitivity by a factor of $\Gamma=L/(n^3b)$ [18], where n is the refractive index of the film. A typical sensitivity enhancement for our experiment is $\Gamma\sim100$.

The initial work with waveguide THz-TDS measured 20 nm layers of water which were deposited in-situ within the waveguide [15]. Recently, we have extended this technique to organic polycrystalline thin films [16, 19], formed on the waveguide metal plate either by drop casting or sublimation. In contrast to the disordered pellets, the resulting polycrystalline thin film is ordered with respect to the plate surface (and hence to the THz polarization). This ordering has the important effect of strongly reducing the inhomogeneous broadening, resulting in significantly narrower lines (and possibly revealing new features), particularly at cryogenic temperatures. Waveguide THz-TDS has been demonstrated with 1,2- and 1,3-dicyanobenzene [16, 19], TCNQ [19], several small biological molecules [20], as well as aspirin and four related compounds [21].

In general, one obtains line sharpening upon cooling until the homogeneous broadening is below the residual inhomogeneous broadening due to disorder in the sample. For example, at very low tempertures (< 10 K), the full linewidths of Raman active low frequency vibrations of highly crystalline molecular solids can be on the order of 1 GHz [22]. In our previous work [16, 19-21], we could only cool our pellets and waveguides to liquid nitrogen temperature (77 K). Due to the large disorder in pellets, further cooling using conventional THz-TDS has little effect [11, 12].

However, we have recently found that further cooling below liquid nitrogen temperature has a very large effect when using the ordered films of waveguide THz-TDS. The additional sharpening with further cooling implies that our polycrystalline thin films have very strong planar order (i.e. the crystals are well aligned to the metal surface) and with the individual microcrystals containing a high degree of crystallinity. We can therefore obtain measurements approaching the quality of single crystals, but with the easy to prepare polycrystalline films.

In this paper we extend waveguide THz-TDS to temperatures as low as 11 K and demonstrate a dramatic sharpening of THz vibrational modes. This line narrowing effect reveals a rich vibrational structure that underlies a crystalline organic solid. The materials studied here are the explosives related solids, 2,4-dinitrotoluene (2,4-DNT) and 2,6-dinitrotoluene (2,6-DNT). As shown in Fig. 1, these materials are closely related to the explosive 2,4,6-trinitroluene (2,4,6-TNT). Our waveguide THz-TDS measurements at temperatures as low as 11 K have resulted in the narrowest linewidths and the most highly resolved THz vibrational fingerprint spectra observed to date for an explosives related solid.

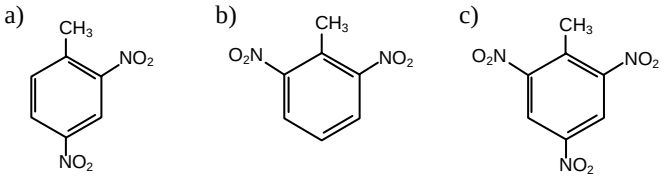

Fig 1. Chemical structures of: a) 2,4-DNT, b) 2,6-DNT, c) 2,4,6-TNT

2. Experimental apparatus

We measured the THz spectra of both 2,4- and 2,6-DNT using THz-TDS of pellets and waveguide THz-TDS of ordered polycrystalline films. Both techniques are illustrated in Fig. 2. For conventional THz-TDS, a pellet of either 2,4- or 2,6-DNT mixed with polyethylene

#92514 - $15.00 USD Received 6 Feb 2008; revised 7 Mar 2008; accepted 7 Mar 2008; published 11 Mar 2008

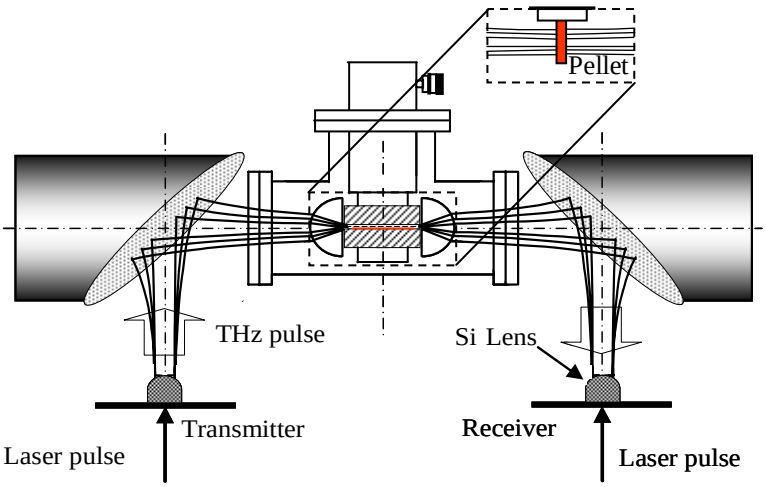

Fig 2. Waveguide THz-TDS. Inset indicates replacement of waveguide with pellet for conventional THz-TDS.

was placed in the standard THz-TDS apparatus [23, 24]. THz radiation is generated by a photoconductive antenna which is driven by an ultrafast laser pulse. This radiation is collimated, transmitted through the pellet, and subsequently focused and detected by another photoconductive antenna. Unlike previous work on DNT, our pellets are cooled by a two stage He cryocooler to approximately 12 K, as measured by a Si diode mounted on the pellet holder, in order to minimize homogenous broadening.

For this application of waveguide THz-TDS, the waveguides were constructed from two Al plates with a length of 30 mm, separated by spacers defining a gap of 50 μm. THz pulses are coupled into and out of these waveguides via high-resistivity Si cylindrical lenses. The amplitude transmission of an empty Al waveguide (50 μm gap) can be as high as 20% at 1 THz, dropping to 5% at 4 THz. This, along with the lack of dispersion, results in a reasonably large signal over a very wide bandwidth. Similarly to the pellets, the waveguides were also cooled to 12 K.

Our instrument resolution is determined by the maximum temporal scan length before encountering a strong reflection, as shown in Fig. 3. For the pellet experiments, the first reflection at 30 ps is due to the pellet itself. However, this reflection is weak due to the low index n~1.5 for polyethylene and the additional double pass through the absorptive pellet, inducing only minor Fabry-Perot oscillations on the amplitude spectrum. The first strong reflection is due to the 10 mm thick Si windows (with the high index of n~3.4) of the vacuum chamber and occurs at 227 ps, corresponding to a frequency resolution of 4.4 GHz (0.15 cm^{-1}). This is not a concern for the relatively broad linewidths observed with the pellet. Typically, scan lengths of 67 ps were used for the pellet measurements. For the waveguide, the first strong reflection is due to the 6.56 mm thick high-resistivity Si coupling lenses, and occurs at 150 ps, corresponding to a spectral resolution of 6.7 GHz (0.22 cm^{-1}). Given the very narrow linewidths seen with the waveguide, this spectral resolution can be a limiting factor. The ringing after the main pulse is pronounced for the waveguide with measurable information continuing to the reflection at 150 ps, while the corresponding ringing for the pellet decays below the noise floor before the end of the scan. For most of the measurements, 4 scans were averaged in order to improve the signal to noise (S/N) ratio. The exception was the 2,4-DNT waveguide measurement at 11 K, where 12 scans were averaged. All scans were zero-padded before taking a numerical Fourier transform.

In the case of both the pellet and the waveguide, a reference A_{ref} is estimated by fitting the amplitude spectra A_{spec} at points away from any sharp features with a spline. The amplitude absorbance is then calculated via the expression: Absorbance = $-\ln[A_{spec}/A_{ref}]$.

#92514 - $15.00 USD Received 6 Feb 2008; revised 7 Mar 2008; accepted 7 Mar 2008; published 11 Mar 2008

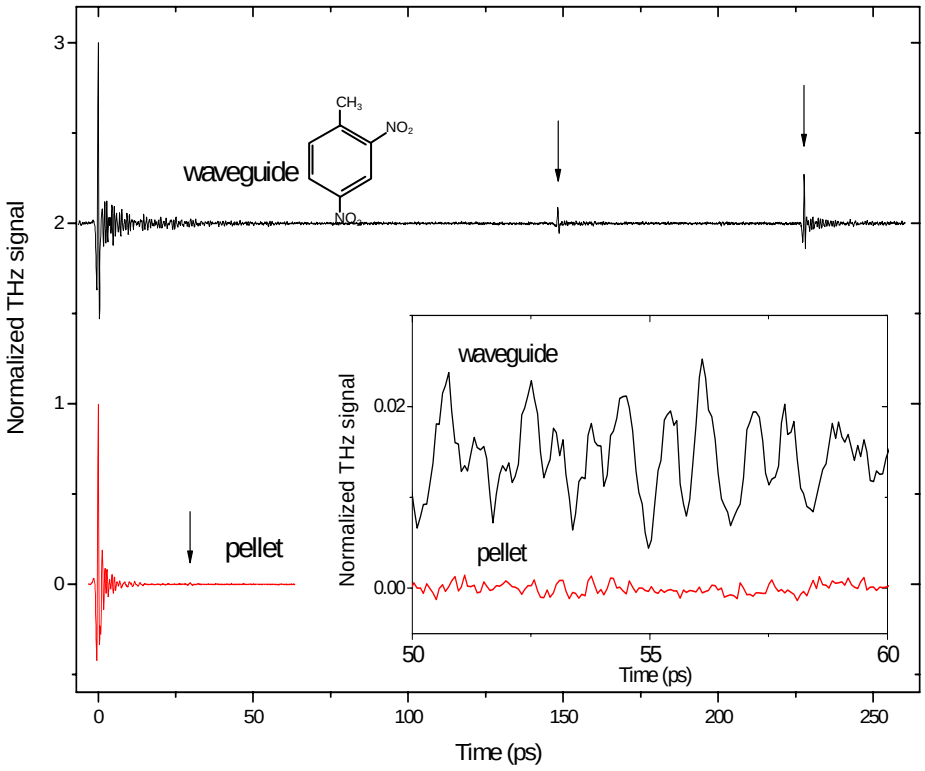

Fig 3. Normalized THz pulses transmitted through 2,4-DNT pellet and waveguide at 11 K. Inset shows pulses trailing edges at times of 50 through 60 ps. THz pulses transmitted through waveguide are offset for clarity. Reflection at 30 ps is due to pellet. Reflections at 150 ps and at 227 ps are due to Si lenses and windows respectively.

3. Results and discussion

The center frequencies and amplitude full-width-at-half-maximum (FWHM) linewidths (indicated in parentheses) of the observed spectral features at the indicated temperatures for both the 2,4- and 2,6-DNT with both pellets and waveguides are summarized in table 1. These include the many new features observed with waveguide THz-TDS. For the purpose of comparison, the observed features in previous work [3,6-9] is also included in this table.

3.1 2,4-DNT

The 2,4-DNT pellet is comprised of 32 mg DNT and 330 mg of polyethylene mixed powders and is formed at a pressure of 11 metric tonnes. It has a diameter of 12.5 mm and a thickness of 3 mm. The amplitude spectra of the transmitted THz as a function of temperature is shown in Fig. 4. The features sharpen upon cooling, with only a minor change below 80 K, resulting in 7 observable features at 11 K. The features also blue shift during cooling, possibly due to the anharmonicity of the vibrational modes.

#92514 - $15.00 USD Received 6 Feb 2008; revised 7 Mar 2008; accepted 7 Mar 2008; published 11 Mar 2008

Table 1. Comparison of center line frequencies in THz[a] of 2,4-DNT for this work and references 3, 6, 8 and 9.

This work waveguide 11 K (2,4-DNT) 12 K (2,6-DNT)	This work pellet 11 K (2,4-DNT) 13 K (2,6-DNT)	This work pellet 293 K	Ref 3 pellet 293 K	Ref 6 pellet 293 K	Ref 7 pellet 293 K	Ref 8 pellet 293 K	Ref 9 pellet 293 K
2,4-DNT							
0.58 (0.008)	0.55 (0.034)		0.43	0.43			
0.62 (0.010)	0.63 (0.045)		0.66	0.66			
0.88 (0.007)							
1.06 (0.007)	1.07 (0.11)						
1.12 (0.014)							
1.22 (0.043)	1.20 (0.08)	1.06 (0.18)	1.08	1.08		1.08	1.08
1.24 (0.010)							
1.46 (0.008)	1.46 (0.10)			1.36			
1.62 (0.012)	1.60 (0.13)						
1.65 (0.018)							
1.70 (0.010)							
1.89 (0.008)							
1.95 (0.015)	1.92 (0.24)						
2.03 (0.017)							
2.22 (0.009)							
2.48 (0.05)							
2.77 (0.04)							
3.02 (0.13)			2.52	2.54	2.52		
3.46 (0.15)							
2,6-DNT							
1.18 (0.012)	1.17 (0.08)	1.10 (0.21)	1.10	1.10	1.10		
1.52 (0.008)	1.49 (0.06)	1.35 (0.38)	1.35	1.36	1.37		
1.68 (0.009)	1.62 (0.06)	1.56 (0.23)	1.56	1.58	1.57		
1.80 (0.008)	1.76 (0.06)						
1.83 (0.007)	1.80 (0.03)						
2.10 (0.012)							
			2.50	2.50			

[a]FWHM linewidths in THz in brackets

#92514 - $15.00 USD Received 6 Feb 2008; revised 7 Mar 2008; accepted 7 Mar 2008; published 11 Mar 2008

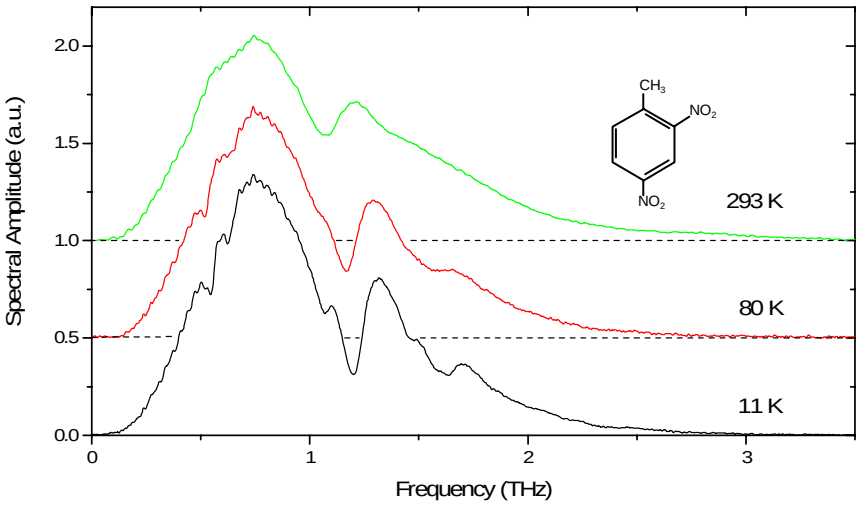

Fig. 4. Amplitude Spectra of THz transmitted through 2,4-DNT pellet as a function of temperature. Spectra at 80 K and 293 K are offset for clarity.

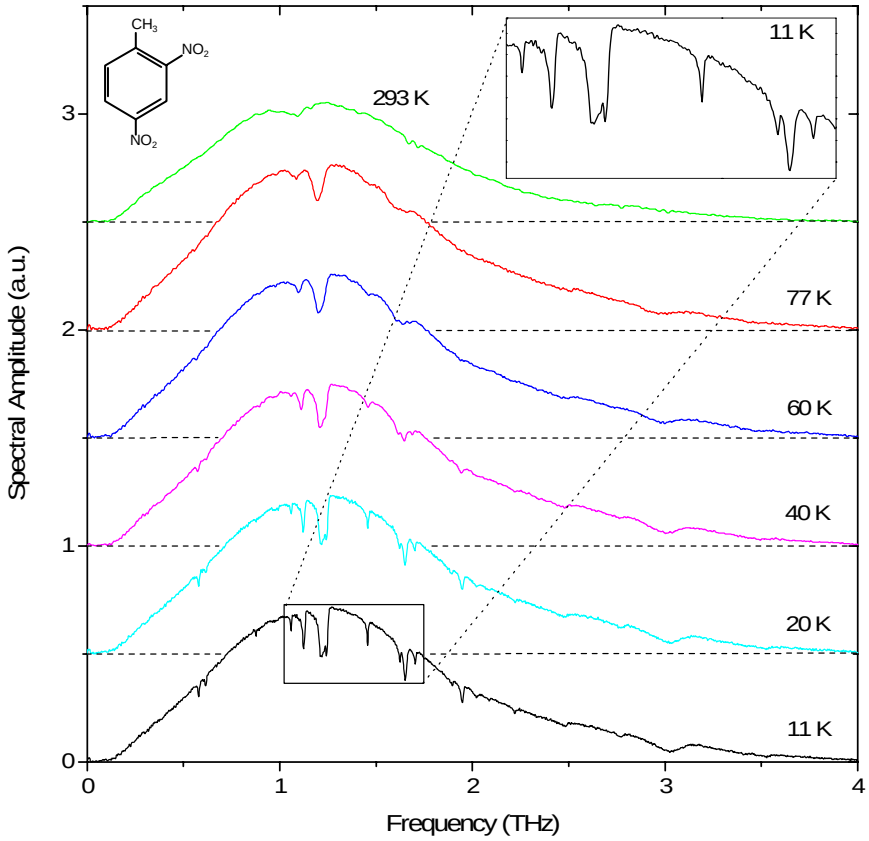

Fig. 5. Amplitude spectra of THz transmitted through 2,4-DNT waveguide as a function of temperature. Spectra at 20 K through 293 K are offset for clarity. Inset shows detail of 11 K spectrum.

#92514 - $15.00 USD Received 6 Feb 2008; revised 7 Mar 2008; accepted 7 Mar 2008; published 11 Mar 2008

The 2,4-DNT waveguide film was formed by drop casting 100 µl of a 2.5 mg/ml acetone solution onto a polished Al plate. The relatively thick edges were removed by a solvent soaked swab, resulting in a visibly uniform film with an estimated mass of less than 100 µg, compared to 32 mg of DNT used for the pellet sample. The amplitude spectra of the transmitted THz through the waveguide as a function of temperature are shown in Fig. 5. Similarly to the pellet, the features both sharpen and blue-shift at lower temperatures. In sharp contrast to the pellet, there is substantial sharpening of the features at lower temperatures, particularly below 80 K. At 11 K, this sharpening reveals 19 observable lines. This is nearly 3 times the number of lines observed with the pellet and corresponds to a substantial increase in both the obtainable information about the vibrational modes of this material as well as the precision of their identification.

The amplitude absorbance of both the 2,4-DNT pellet and waveguide at 11 K is shown in Fig. 6. Using the waveguide, the doublet near 1.1 THz, the doublet near 1.5 THz and the broad feature near 1.9 THz has been resolved into four lines each, corresponding to a narrowing by a factor of 5, 10 and 20, respectively. In addition, the 0.58 and 0.68 THz lines are approximately 4 times narrower than for the pellet. Furthermore, lines at 0.88, 2.22, 2.48,

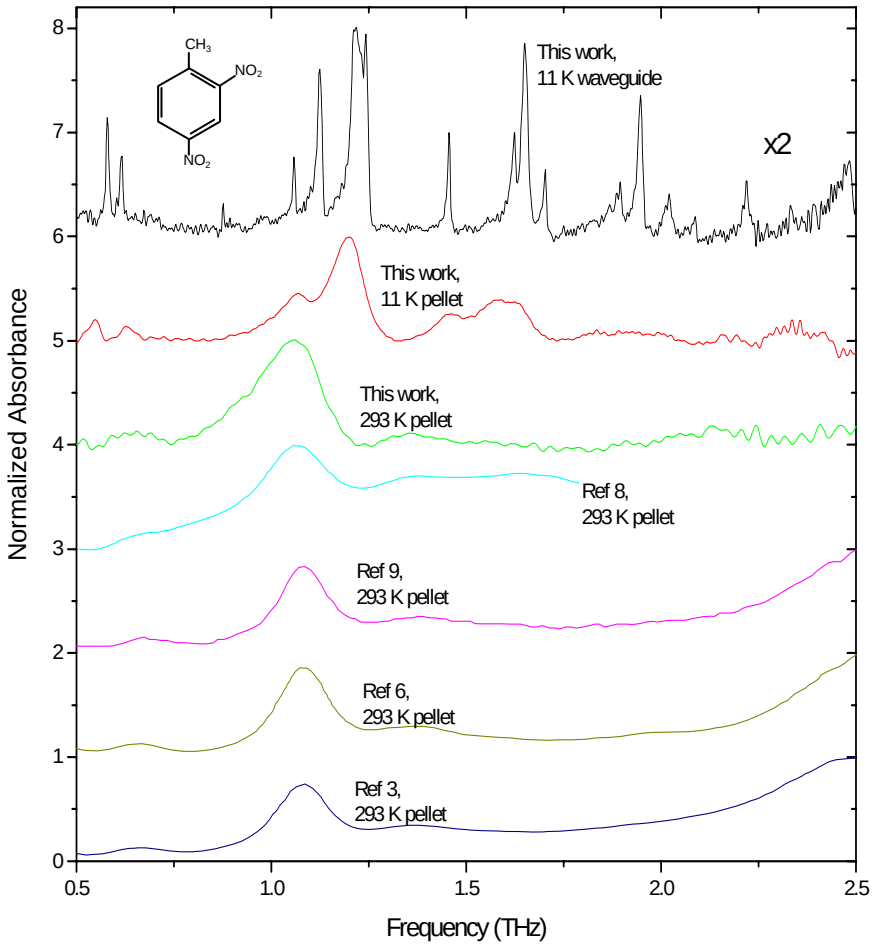

Fig. 6. Normalized amplitude absorbance of 2,4-DNT waveguide at 11 K, 2,4-DNT pellet at 11 K and 293 K and 2,4-DNT pellet at 293 K for Ref 3, 6, 8 and 9. The pellet for this work contained 32 mg of 2,4-DNT, whereas the waveguide film contains less than 100 µg of 2,4-DNT. The estimated signal-to-noise ratio for the waveguide measurement is ~10:1 at 0.5 THz, ~70:1 at 1.2 THz and ~8:1 at 2.5 THz. The curves are normalized to unity with the exception of the 11 K waveguide data, which is normalized to two for better visibility.

#92514 - $15.00 USD Received 6 Feb 2008; revised 7 Mar 2008; accepted 7 Mar 2008; published 11 Mar 2008

2.77, 3.02 and 3.46 THz are sufficiently sharp to be observed with the waveguide. Of the 19 lines, 11 have a measured linewidth of less than 15 GHz (0.5 cm^{-1}). Given the instrument resolution of 6.7 GHz (0.22 cm^{-1}), the intrinsic linewidths will be smaller.

Figure 6 also compares the normalized absorbance of the 2,4-DNT pellet and waveguide in this work to the previously measured absorbance with room temperature pellets[3, 6, 8, 9]. This comparison is also shown in table 1. Previous work has measured up to five broad features in this frequency range, compared to the 19 narrow lines measured in this work with the low temperature waveguide.

The increased resolution of the waveguide spectrum compared to the pellet is due to the planar order of the polycrystalline film on the metal waveguide plate. An optical micrograph of the ordered polycrystalline film is shown in Fig 7. X-ray analysis of the film has revealed a strong orientation on the (001) plane. 2,4-DNT has been shown to crystallize in the $P2_1/n$ space group with eight molecules per unit cell [25]. Density functional theory of an isolated molecule [8] has attributed the modes in this frequency range to phonons. There are 6B-3 phonon modes predicted for a unit cell containing B molecules, thus for 2,4-DNT 45 phonon modes are anticipated with 21 being infrared active. Furthermore, low frequency intramolecular vibrations (which may differ between a crystal and an isolated molecule) will also occur in the THz region. Given these material properties for 2,4-DNT, it is not surprising the 19 vibrational modes are revealed at low temperature for the waveguide film when inhomogeneous broadening effects are suppressed. It's possible that high precision THz measurements such as provided here can help refine theoretical modeling [26, 27] of THz vibrational spectra in the crystalline state.

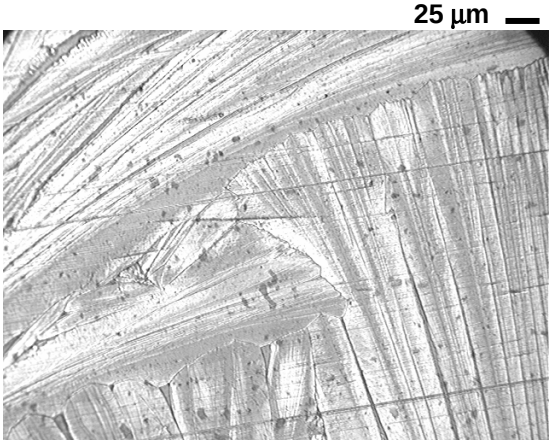

Fig. 7. Optical micrograph of 2,4-DNT film on Al waveguide plate.

3.2 2,6-DNT

The 2,6-DNT pellet is comprised of 62 mg of DNT and 330 mg of polyethylene, while the 2,6-DNT waveguide film was formed by drop casting 100 μl of a 10 mg/ml acetone solution onto a polished Al plate. The estimated mass of the film on the waveguide plate is less than 1 mg. The amplitude spectra of the transmitted THz through the 2,6-DNT pellet as a function of temperature is seen in Fig. 8. Similarly to the 2,4-DNT pellet, there is minor sharpening of features upon cooling with very little change below 80 K.

The amplitude spectra of the transmitted THz through the 2,6-DNT waveguide as a function of temperature is seen in Fig. 9. Similarly to the 2,4-DNT waveguide, there is a large amount of sharpening upon cooling, particularly below 80 K. Unlike the 2,4-DNT waveguide, there is no additional splitting of the features, with a total of six lines observed at 13 K. The broad, temperature independent feature at 1.8 THz is considered to be due to the waveguide itself and not to the 2,6-DNT.

#92514 - $15.00 USD Received 6 Feb 2008; revised 7 Mar 2008; accepted 7 Mar 2008; published 11 Mar 2008

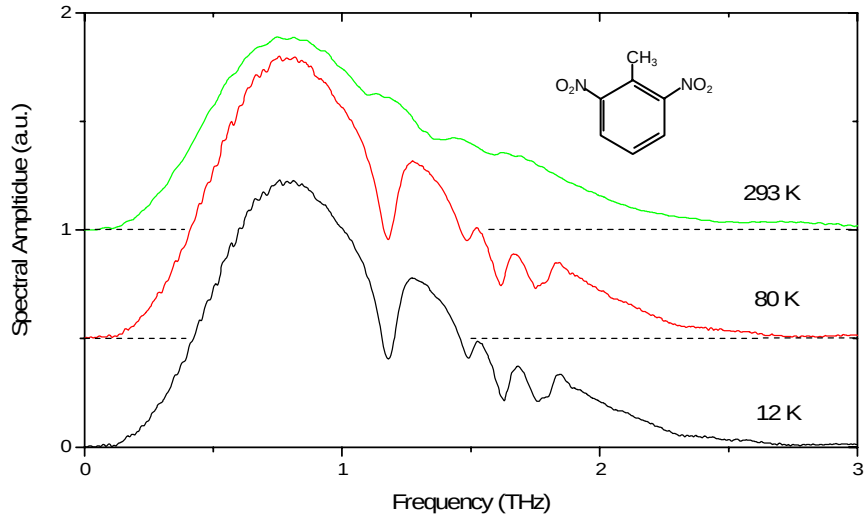

Fig. 8. Amplitude spectra of THz transmitted through 2,6-DNT pellet as a function of temperature. Spectra at 80 K and 293 K are offset for clarity

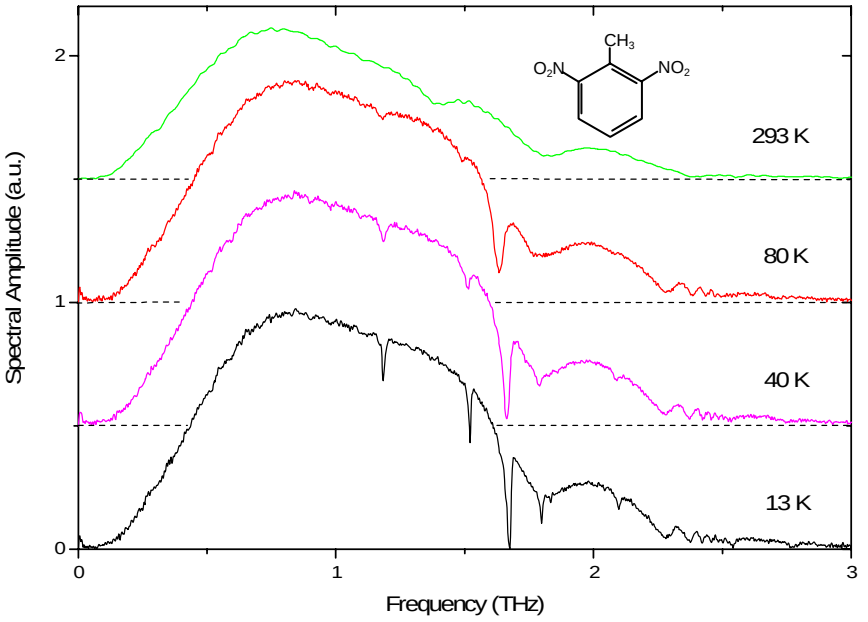

Fig. 9. Amplitude spectra of THz transmitted through 2,6-DNT waveguide as a function of temperature. Spectra at 40 K through 293 K are offset for clarity.

The amplitude absorbance of both the 2,6-DNT pellet and waveguide at approximately 12 K is shown in Fig. 10. In addition, the absorbance measured in this work is compared to previous work [3, 6, 7] with room temperature pellets in both Fig. 10 and Table 1. The absorption features are considerably sharper with the waveguide compared to the pellet, with linewidths being approximately 7 times narrower for the waveguide. One additional line at 2.10 THz can be observed with the waveguide. All six of the observed lines with the waveguide have a measured linewidth less than 15 GHz (0.5 cm^{-1}), implying that the actual linewidth is even smaller. The dramatic increase in the relative absorption strength of the 1.68 THz line may be due to the dipole moment of this vibrational mode being well aligned with the THz polarization in the waveguide. The center line frequency and linewidth of this

#92514 - $15.00 USD Received 6 Feb 2008; revised 7 Mar 2008; accepted 7 Mar 2008; published 11 Mar 2008

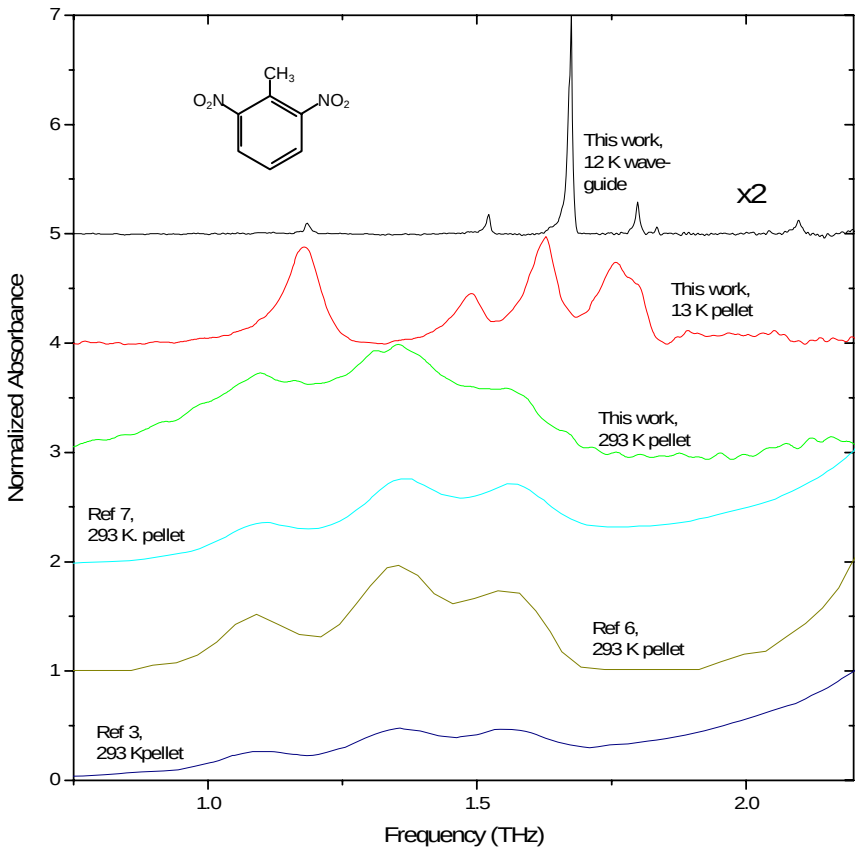

Fig. 10. Normalized amplitude absorbance of 2,6-DNT waveguide at 12 K, 2,6-DNT pellet at 13 K and 293 K and 2,6-DNT pellet at 293 K for Ref 3, 6 and 7. The estimated signal-to-noise ratio for the waveguide measurement is ~40:1 at 1.18 and 1.68 THz and ~20:1 at 2.10 THz. The curves are normalized to unity with the exception of the 12 K waveguide data, which is normalized to two for better visibility.

relatively isolated line as a function of temperature for both the pellet and the waveguide is shown in Fig. 11. Note that both the degree of blue-shifting and line narrowing is considerably greater for the waveguide, particularly at lower temperatures.

The second 2,6-DNT line (1.35 THz at 293 K) has been attributed [7] to the torsion of the NO_2 groups, while the other lines have been attributed to phonon modes. The observation of fewer spectral features for 2,6-DNT compared to 2,4-DNT may be partly due to its crystallization in a different space group, $P2_12_12_1$ [28], with four molecules per unit cell. There are 21 phonon modes predicted for this simpler crystal structure, only 9 of which are infrared active.

4. Conclusions

Waveguide THz-TDS has been used to obtain high resolution, narrow-line, high sensitivity spectral measurements of the vibrational modes of the explosive related solids 2,4- and 2,6-DNT.

The waveguide measurement of 2,4-DNT is particularly impressive with a number of features splitting upon cooling to 11K, for a total of 19 observed lines between 0.58 and 3.46 THz. Previous work with room temperature 2,4-DNT pellets [3, 6, 8, 9] have observed no more than five lines in this frequency range. Of our 19 observed lines, 11 have a FWHM linewidth of less than 15 GHz (0.5 cm^{-1}). The spectrum of a 2,4-DNT pellet undergoes little

#92514 - $15.00 USD Received 6 Feb 2008; revised 7 Mar 2008; accepted 7 Mar 2008; published 11 Mar 2008

sharpening under cooling with seven observed lines. The median linewidth of the waveguide spectra is approximately 8 times sharper than the median linewidth of the pellet spectra.

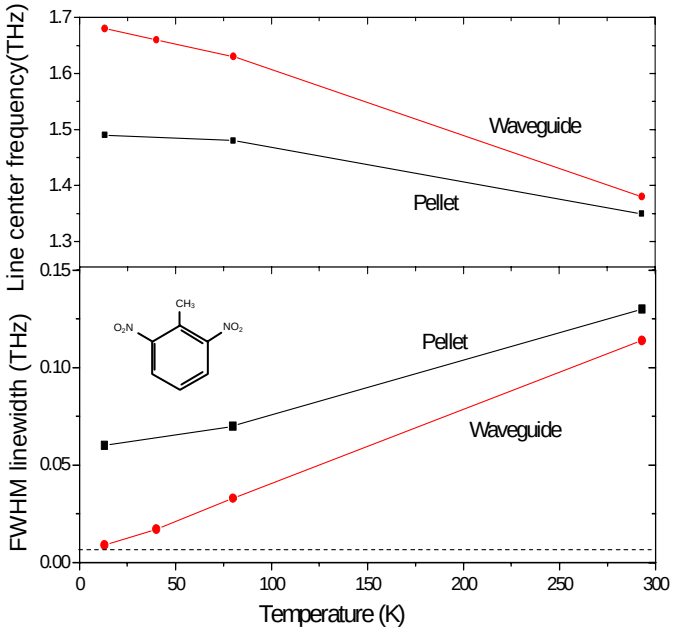

Fig. 11. Center line frequency and FWHM linewidth for the strongest line in 2,6-DNT pellet and waveguide. The dashed line corresponds to the 6.7 GHz instrument resolution.

The waveguide spectrum of 2,6-DNT also sharpens significantly under cooling, with all six observed lines having a linewidth of less than 15 GHz at 13 K. The pellet spectrum undergoes only minor sharpening under cooling. The median linewidth of the waveguide spectra is approximately 7 times sharper compared to the pellet.

The line narrowing effect observed for the waveguide films is related to the formation of micro-crystals with high crystalline quality. For the 2,4-DNT film, crystallinity was confirmed by the observation of a sharp x-ray diffraction pattern, which also indicated a preferred orientation of the microcrystals, where the (001) plane of the unit cell is parallel to the metal surface. To date, the drop casting method has been the most effective in producing high quality films. The detailed film morphology depends on a variety of preparation conditions, including solute concentration, solvent, and surface quality of the metal. For relatively small organic molecules such as the dinitrotoluenes, tetracyanoquindimethane [19], and aspirin derivatives [21], we have found generally better and more reproducible film formation on plasma cleaned, polished metal surfaces. When cast from non-aqueous solvents these small molecules have tended to form films of similar quality on aluminum, gold, and copper surfaces. In contrast, bio-organic molecules that are more flexible and with hydrogen-bonding interactions tend to form films with more variation in crystalline quality. For some bio-organics we have observed a strong dependence on the type of metal surface used [20].

In addition, the technique of waveguide THz-TDS is approximately 100 times more sensitive than conventional THz-TDS with a pellet. This allows one to use considerably less material. This can be useful when measuring dangerous materials such as explosives.

Acknowledgments

We would like to thank Aihau Xie for the loan of the He cryocooler. This work was supported by the National Science Foundation and the Office of Naval Research.

#92514 - $15.00 USD Received 6 Feb 2008; revised 7 Mar 2008; accepted 7 Mar 2008; published 11 Mar 2008